Screening, charge distribution, and electron correlations in metallic alloys

V. Drchal[*]

Institute of Physics, AS CR, Na Slovance 2, CZ-182 21 Praha 8, Czech Republic

R. Hammerling and P. Weinberger

Center for Computational Materials Science, Technical University of Vienna, Getreidemarkt 9/134, A-1060 Vienna, Austria

We study a model of charge transfer in alloys proposed by Bruno, Zingales, and Wang [Phys. Rev. Lett. **91**, 166401 (2003)] and show its connection with electron-electron correlations. We then investigate in detail the properties of Madelung and related matrices, the mechanism leading to the screening of the electrostatic interactions between atomic net charges in random alloys, and calculate the screened interactions. Furthermore, we derive an expression for the total energy and show that the fluctuation contributions to the local and Madelung energy mutually cancel. We then derive and discuss the probability distribution function of local charges and make a comparison with calculations for large supercells. Finally, we discuss the relation of the present approach to other theories aimed at the description of Coulomb effects in alloys.

I. INTRODUCTION

There are two important and difficult problems in an *ab initio* theory of disordered alloys, namely, (i) the effect of different sizes of the constituent atoms, which in turn leads to local strains and structural deformations, and (ii) the charge transfer between different atomic species and the screening of electrostatic interactions.

Here we wish to concentrate on the charge transfer and screening phenomena. These, as it was criticized by Magri *et al.*,[1] are neglected in the isomorphous model of alloys in which it is assumed that the net charges q^Q and the Madelung potentials V^Q are identical for all atoms of type Q. Several attempts were made to include Coulomb effects within the isomorphous model. The screened impurity model (SIM),[2] which is based on calculations[3] for a single impurity in an otherwise perfect metallic host, showed that the charge on an impurity site is screened approximately within the first coordination shell. In the SIM, each atom in the alloy is surrounded by a screening charge located at the radius R_1 of the first coordination shell, which completely screens the charge of the atom. As a result, an additional term (the so-called local Madelung correction) is added to the potential. The corresponding contribution to the total energy is often considered to be insufficient and for practical purposes is multiplied by a correction factor β. A closely related method is the screened CPA (Ref. 4) that differs from the SIM by setting $\beta=1$.

The charge-correlated (CC) CPA is based on the observation that the charge on an atom is approximately proportional to the difference between numbers of like and unlike atoms in the first coordination shell.[4] This leads quite naturally to the polymorphous model of an alloy[5] in which each atom of type Q is characterized by individual values of q_i^Q and V_i^Q that depend on its environment due to the electrostatic field and electronic structure effects beyond the single-site approximation.

The charge-transfer problem can be circumvented by employing neutral atomic spheres.[6] In this method, the atomic radii are changed so as to achieve vanishing net charges under the condition of constant total volume of the alloy. This scheme works well for small charge transfer, but with increasing charge transfer the necessary changes of the atomic radii become too large, which leads to uneven overlaps between the spheres and a loss of accuracy.

A reliable and detailed information on the charge transfer and electrostatic potentials in alloys is provided by calculations for large supercells that serve as models of alloys. The locally self-consistent multiple scattering (LSMS)[7] and locally self-consistent Green's function[8] (LSGF) methods were used to treat supercells containing hundreds and even thousands of atoms.

Detailed studies of screening in alloys based on the LSGF calculations and using the concept of the screening charge[9,10] have shown that the results of the single-site CPA are almost identical to those of the LSGF with a single-site interaction zone and that the screening is universal, i.e., it is almost independent of the alloy composition, lattice spacing, and crystal structure. Intersite-screened Coulomb interaction that should be added to the effective pair interaction calculated within the generalized perturbation method (GPM) were derived. It was shown that a correct description of local environment effects requires one to account for multipole electrostatic interactions beyond the atomic-sphere and single-site approximations.

One of the important results of the supercell calculations is the linear relationship between the net charge and Madelung potential[11] at a lattice site i,

$$a_i q_i + V_i = k_i, \qquad (1)$$

the so-called qV relation. Here, a_i and k_i are constants that depend on the type of atom-occupying site i, i.e., they assume the values a^A or a^B and k^A or k^B, respectively, and are almost independent of the alloy concentration. The constants a^Q and k^Q can be derived from the results for large supercells or from local-field CPA calculations.[12] Although relation (1) is fulfilled with a good accuracy, it need not be valid in general. For details, see Ref. 9.

In order to achieve a better understanding of the charge transfer and screening in alloys, Bruno, Zingales, and Wang[13] (BZW) proposed a simple phenomenological model, which captures rather well the main features of these phenomena. The expression for the energy connected with the distribution of local net charges $[q_i]$ in a binary random alloy A_xB_y ($y=1-x$) reads

$$E([q_i]) = E^{\text{loc}}([q_i]) + E^{\text{Mad}}([q_i])$$
$$= \frac{1}{2}\sum_i a_i(q_i - b_i)^2 + \frac{1}{2}\sum_{i,j} M_{ij}q_iq_j, \qquad (2)$$

where the parameters a_i are closely connected to the strength of electron-electron interactions, $b_i = k_i/a_i$ are bare net charges of atom i, and

$$M_{ij} = \begin{cases} e^2/R_{ij} & \text{for } i \neq j \\ 0 & \text{for } i = j, \end{cases} \qquad (3)$$

are elements of the Madelung matrix.

In this paper we wish to investigate the properties of the BZW model in more detail. The paper is organized as follows: in Sec. II we develop the theoretical description including the properties of Madelung and related matrices and screening of on-site and intersite Madelung interactions. In Sec. II we also present the statistics of local charges and derive an improved expression for the Madelung energy. In Sec. III we present a comparison with the supercell calculations of Ref. 14, and in Sec. IV we discuss the approximate treatments of charge transfer in SIM and CCM. The Appendix contains a derivation of screened Madelung interactions (Appendix A).

II. THEORY

The admissible values of net charges q_i may be limited by the inequalities $q_i^{\min} \leq q_i \leq q_i^{\max}$. The requirement of the charge neutrality

$$\sum_i q_i = 0 \qquad (4)$$

could be accounted for by introducing a Lagrange multiplier λ,

$$\Psi([q],\lambda) = E - \lambda\sum_i q_i, \qquad (5)$$

as was done in Ref. 13, but, as we will see later, this is a superfluous complication and need not be introduced. The charge neutrality is fulfilled automatically due to the long-range character of the electrostatic interactions because the charged system always has a higher energy than the neutral system.

The minimization of Eq. (2) with respect to the charge field $[q_i]$ leads to a set of equations,

$$a_i(q_i - b_i) + \sum_j M_{ij}q_j = 0, \qquad (6)$$

the solution thereof is given by

$$q_i = \sum_j G_{ij}a_jb_j, \qquad (7)$$

where G is defined as

$$G = H^{-1}, \quad H = A + M, \quad A_{ij} = a_i\delta_{i,j}, \quad H_{ij} = a_i\delta_{i,j} + M_{ij}. \qquad (8)$$

The matrix H is the Hessian of the energy [Eq. (2)], and the matrix G is, in fact, the resolvent $G(z) = (H-z)^{-1}$ of H calculated at $z=0$. (Note that Bruno *et al.*[13] denote this matrix as Λ.) The model is very similar to a one-particle single-band tight-binding theory of the electronic structure with the Hessian H playing the role of a model Hamiltonian.

A. Properties of the Madelung and related matrices

The Madelung matrix (3) is a real symmetric matrix and thus its eigenvalues are real. It depends on the difference $R_{ij} = |\mathbf{R}_i - \mathbf{R}_j|$ only, so its lattice Fourier transform is given by

$$M(\mathbf{k}) = \sum_i e^{i\mathbf{k}(\mathbf{R}_i - \mathbf{R}_j)}M_{ij}, \qquad (9)$$

and the back transform by

$$M_{ij} = \frac{1}{\Omega_{(\text{BZ})}}\int_{(\text{BZ})} d^3\mathbf{k} \, e^{-i\mathbf{k}(\mathbf{R}_i - \mathbf{R}_j)}M(\mathbf{k}), \qquad (10)$$

where Ω_{BZ} is the volume of the first Brillouin zone. The lattice Fourier transform $M(\mathbf{k})$ can be found with high accuracy by employing the Ewald summation technique,[15] which leads to

$$e^{-2}M(\mathbf{k}) = \sum_{\mathbf{R}\neq\mathbf{0}} \frac{\exp(i\mathbf{k}\mathbf{R})}{|\mathbf{R}|}$$
$$= -\frac{1}{\rho\sqrt{\pi}} + \frac{4\pi}{\Omega_0}\sum_{\mathbf{K}} \frac{\exp\{-[\rho(\mathbf{k}+\mathbf{K})]^2\}}{|\mathbf{k}+\mathbf{K}|^2}$$
$$+ \sum_{\mathbf{R}\neq\mathbf{0}} \exp(i\mathbf{k}\mathbf{R})\frac{\text{erfc}[|\mathbf{R}|/(2\rho)]}{|\mathbf{R}|}, \qquad (11)$$

where Ω_0 is the volume of an elementary cell, $\mathbf{K}$ denotes lattice vectors of the reciprocal lattice, and the optimal value of ρ is $\rho = \Omega_0^{1/3}/(2\sqrt{\pi})$.

For $|\mathbf{k}| \to 0$ $M(\mathbf{k})$ diverges as

$$M(\mathbf{k}) \approx \frac{4\pi}{\Omega_0}\frac{1}{|\mathbf{k}|^2}. \qquad (12)$$

The spectral density,

$$n(x) = \frac{1}{\Omega_{(\text{BZ})}}\int_{(\text{BZ})} d^3\mathbf{k}\,\delta[x - M(\mathbf{k})], \qquad (13)$$

thus extends to $+\infty$ and has a tail (for $x \gg 1$) as follows

$$n(x) \approx \frac{2}{\sqrt{\pi}\Omega_0}x^{-5/2}. \qquad (14)$$

We can partition $M(\mathbf{k})$ into a divergent and a finite part,
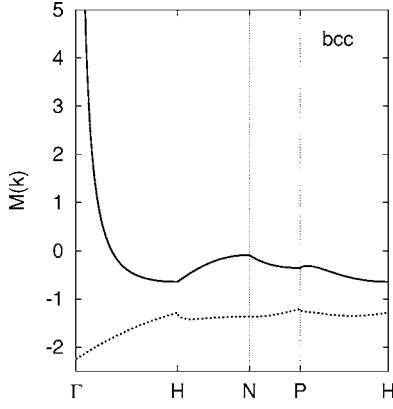
FIG. 1. Spectrum of the Madelung matrix along rays between points of higher symmetry in the Brillouin zone for the bcc lattice. The full line denotes $M(\mathbf{k})$, the broken line $m(\mathbf{k})$.

$$M(\mathbf{k}) = \frac{4\pi}{\Omega_0}\frac{1}{\mathbf{k}^2} + m(\mathbf{k}). \qquad (15)$$

The spectra of the Madelung matrix for the bcc and fcc lattice are shown in Figs. 1 and 2, while the densities of states are shown in Figs. 3 and 4. The minimum of $M(\mathbf{k})$ is attained at $\mathbf{k}_0=(2k_0,k_0,0)$, where $k_0=2\pi\times0.630/a_{\text{fcc}}$ for the fcc lattice, and $\mathbf{k}_0=(k_0,0,0)$, where $k_0=2\pi\times0.794/a_{\text{bcc}}$ for the bcc lattice.

In order to avoid the dependence of calculated quantities on the lattice constant a_{latt} of a particular material, we use the units in which $a_{\text{latt}}=1$, $e^2=1$, and the unit of energy is $\varepsilon_0 = e^2/a_{\text{latt}}$. The relation to Rydberg atomic units is shown by the following example: consider Cu-Zn alloy (Sec. III A) with $a_{\text{latt}}=5.5$ bohrs, $e^2=2$ Ry bohrs. Then $\varepsilon_0=2/5.5$ Ry $=0.3636$ Ry.

The matrix G defined in Eq. (8) fulfills a rather important relation,

$$\sum_j G_{ij} = 0, \qquad (16)$$

which follows from the long-range character of M_{ij} and which will be used several times below. It is derived as follows. The matrix G can be represented as
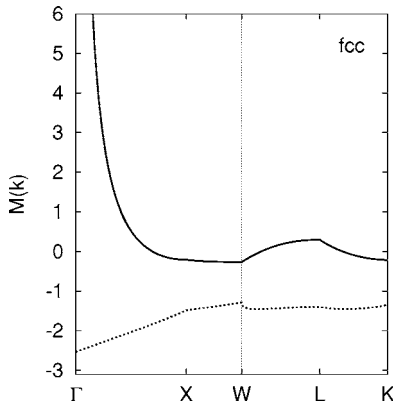

FIG. 2. Spectrum of the Madelung matrix along rays between points of higher symmetry in the Brillouin zone for the fcc lattice. The full line denotes $M(\mathbf{k})$ and the broken line denotes $m(\mathbf{k})$.
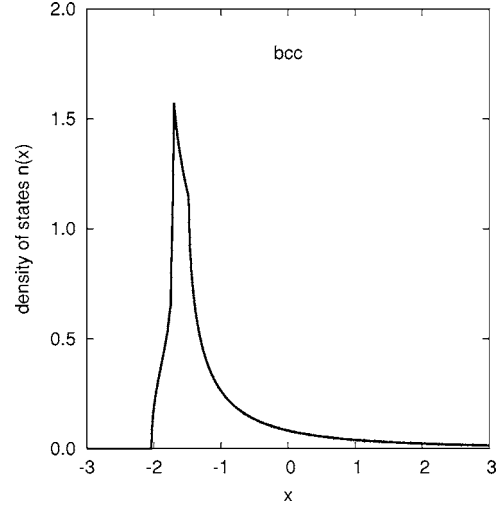

FIG. 3. Spectral density of the Madelung matrix for the bcc lattice as a function of x [see Eq. (13)].

$$G = M^{-1} - GAM^{-1}, \qquad (17)$$

where M^{-1} is given by

$$(M^{-1})_{ij} = \frac{1}{\Omega_{\text{BZ}}}\int_{(\text{BZ})} d^3\mathbf{k}\, e^{-i\mathbf{k}(\mathbf{R}_i-\mathbf{R}_j)}\frac{1}{M(\mathbf{k})}. \qquad (18)$$

Using the relation

$$\sum_j e^{i\mathbf{k}\mathbf{R}_{ij}} = \Omega_{\text{BZ}}\sum_{\mathbf{K}}\delta(\mathbf{k}-\mathbf{K}), \qquad (19)$$

we find

$$\sum_j (M^{-1})_{ij} = \frac{1}{\Omega_{\text{BZ}}}\int_{(\text{BZ})} d^3\mathbf{k}\, \Omega_{\text{BZ}}\sum_{\mathbf{K}}\delta(\mathbf{k}-\mathbf{K})\frac{1}{M(\mathbf{k})} = 0, \qquad (20)$$

because $M(\mathbf{k})$ diverges for $\mathbf{k}\rightarrow0$. Equation (17) written in the site representation then gives
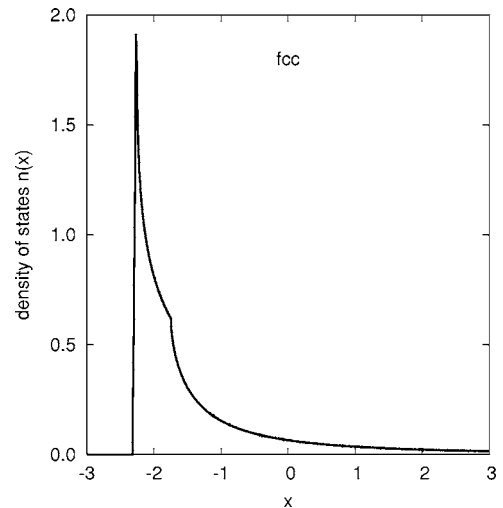

FIG. 4. Spectral density of the Madelung matrix for the fcc lattice as a function of x [see Eq. (13)].

$$\sum_j G_{ij} = \sum_j (M^{-1})_{ij} - \sum_n G_{in} A_{nn} \sum_j (M^{-1})_{nj} = 0, \quad (21)$$

as follows from Eq. (20). The matrix G_{ij} is symmetric, therefore the q_i's calculated from Eq. (7) fulfill the condition (4) automatically.

The energy (2) is a quadratic function of the net charges q_i. The solution (7) of the equation (6) corresponds to a minimum of the energy, if and only if the Hessian H is a positive-definite matrix. The matrix H is positive definite if all its eigenvalues are positive. A sufficient condition is that

$$\min_i a_i + \min_{\mathbf{k}} M(\mathbf{k}) > 0. \quad (22)$$

We will always assume that the matrix H is positive definite. In the opposite case, the minimum of the energy would be attained at the boundary of the admissible region for the q_i's. A good example is an ionic crystal: $q_i \geq b_i$ for cations because a further electron can be removed from a cation only at a high energy cost. Consequently, in purely ionic crystals, $q_i = b_i$ for all sites i.

The Madelung potential

$$V_i = \frac{\partial E^{\text{Mad}}([q_i])}{\partial q_i} = \sum_j M_{ij} q_j, \quad (23)$$

according to Eq. (6), obeys the qV relation

$$a_i q_i + V_i = a_i q_i + \sum_j M_{ij} q_j = a_i b_i = k_i. \quad (24)$$

This is a built-in property of the model in Eq. (2).

B. Randomness of on-site interactions

In general, $a^A \neq a^B$, i.e., the interactions a_i are random. In this case we can use the CPA to calculate the averaged and the conditionally averaged resolvent. Note that the Soven equation has to be solved just for one energy ($z=0$) outside the band. We expect that the CPA is a suitable approximation for our purposes, because we need the overall characteristics of the averaged resolvent, which in turn is well reproduced by the CPA that gives correctly several first moments of the DOS. Moreover, in many alloys the disorder in a_i is rather weak as we will see for the example of Cu-Zn alloys (Sec. III A).

Below we present theoretical results valid for random a_i, however, in some cases, in order to avoid technical details, we resort to the nonrandom approximation $a^A = a^B = a$.

C. Screening of on-site interactions

The strength a_i of local electron-electron interactions can be expressed as a second derivative of the energy (2),

$$a_i = \frac{\partial^2 E([q_i])}{\partial q_i^2}. \quad (25)$$

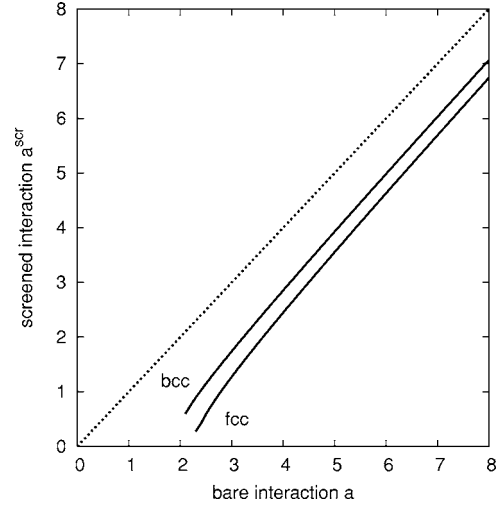This can be compared with a similar formula valid for the Hubbard U,

FIG. 5. The interaction parameter a^{scr} renormalized by the electrostatic interactions with the rest of the system as a function of the bare parameter a. The dotted line corresponds to the absence of screening ($a^{\text{scr}} = a$).

$$E_{\text{int}} = \frac{1}{2} U N(N-1), \quad U = \frac{\partial^2 E_{\text{int}}}{\partial N^2}, \quad (26)$$

where N is the number of interacting particles at a given site. There is, however, an important difference between the a_i and U because U is an effective value diminished by intra-atomic as well as interatomic screening mechanisms, while a_i represents rather a bare value, which is much larger. In other words, the Hubbard U usually describes the interactions between d electrons, while the number of s electrons can change so that the total number of electrons at the atom remains constant,

$$U = E(d^{n+1}s^0) + E(d^{n-1}s^2) - 2E(d^n s^1), \quad (27)$$

while a similar expression for a_i reads as

$$a_i = E(n+1) + E(n-1) - 2E(n), \quad (28)$$

where $E(n)$ is the energy of an atom with n electrons.

Let us fix the value of q_i and then minimize the energy of the system with respect to all other net charges q_j. The energy of the system then becomes a quadratic function of q_i,

$$E_i(q_i) = \min_{q_j, j \neq i} E([q_j]) = E_i + B_i q_i + \tfrac{1}{2} C_i q_i^2. \quad (29)$$

Then it is easy to show (see the Appendix) that the interaction $a_i^{\text{scr}} = C_i$, renormalized by electrostatic interactions with the rest of the system, is given by

$$a_i^{\text{scr}} = 1/G_{ii}. \quad (30)$$

In the case of nonrandom a_i's the renormalized on-site interaction is simply given by

$$a^{\text{scr}} = 1/G_{ii} = \left[\frac{1}{\Omega_{BZ}} \int_{(BZ)} d^3\mathbf{k} \, G(\mathbf{k}) \right]^{-1}. \quad (31)$$

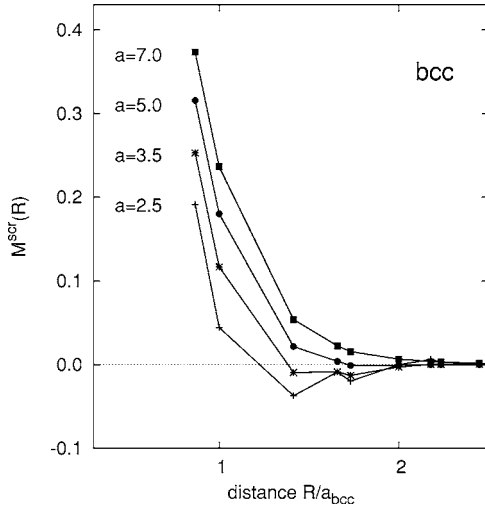The results for the fcc and bcc lattice are shown in Fig. 5.

FIG. 6. Screened electrostatic interactions for the bcc lattice as a function of the distance (in units of the lattice constant a_{lattice}) for the bare interaction parameters of $a=2.5$, 3.5, 5, and 7.

D. Screened electrostatic interactions

The strength $M_{ij}=e^2/R_{ij}$ of the bare electrostatic interaction between the lattice sites i and j with net charges q_i and q_j can be expressed as a second mixed derivative of the energy of the system with respect to q_i and q_j,

$$M_{ij}=e^2/R_{ij}=\frac{\partial^2 E([q_i])}{\partial q_i \partial q_j}, \tag{32}$$

if all other charges are fixed. However, if we allow other charges to relax so as to attain the minimum of the energy similarly as in the Sec. II C, we obtain (see the Appendix) the screened electrostatic interactions (for $i \neq j$),

$$M_{ij}^{\text{scr}}=\frac{\partial^2 E_{ij}([q_i])}{\partial q_i \partial q_j}=-\frac{G_{ij}}{G_{ii}G_{jj}-G_{ij}G_{ji}}, \tag{33}$$

where

$$E_{ij}(q_i,q_j)=\min_{q_k,k\neq i,j} E([q_k]). \tag{34}$$

The screened interactions tend to the bare electrostatic interactions for large values of the interaction parameter a,

$$\lim_{a\to\infty} M_{ij}^{\text{scr}}=M_{ij}. \tag{35}$$

For the case of nonrandom a_i, the screened electrostatic interactions M_{ij}^{scr} are shown in Figs. 6 and 7 as a function of the distance $R=|R_{ij}|$ for $a=2.5$, 3.5, 5, and 7, while in Figs. 8 and 9 they are displayed for the first five neighbors as a function of the interaction strength a. In contrast to the bare electrostatic interactions that depend only on the distance, are positive, and monotonously decrease with distance, the screened interactions (at least for small distances and a small value of the interaction constant a) can acquire negative values, need not be monotonous, for very small values of a the M_{ij}^{scr} can even oscillate (see, e.g., Figs. 6 and 7) and are anisotropic, i.e., they depend on the direction. For large $|\mathbf{R}|$ one can derive an asymptotic formula for M_{ij}^{scr} (see the Ap-

pendix). The screened interactions M_{ij}^{scr} in Fig. 6 for $a=5$ that corresponds to the CuZn alloy compare well with those of Ref. 9, Fig. 8.

If we vary the charge on one site, e.g., q_i, and allow all other charges to relax, then the change of the charge on another site, say j, is given by

$$\delta q_j=\frac{G_{ji}}{G_{ii}}\delta q_i, \tag{36}$$

which follows from Eq. (A7).

The phase stability of alloys is governed by an effective alloy Hamiltonian of Ising type;[16] its parameters are called effective interatomic interactions. The screened electrostatic interactions contribute to the effective interatomic interactions in the following manner:

FIG. 8. Screened electrostatic interactions for the bcc lattice as a function of the bare interaction parameter a for the first five neighbors (indicated explicitly).
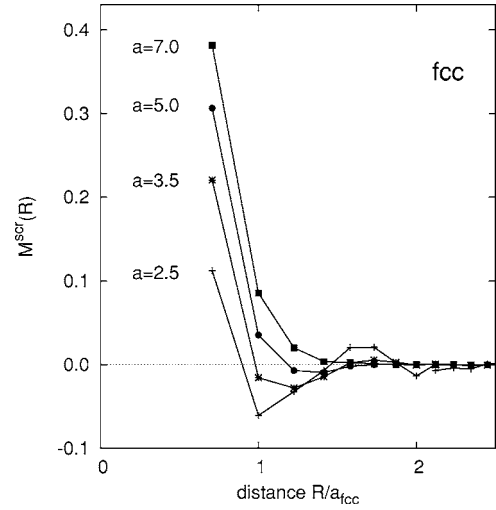

FIG. 7. Screened electrostatic interactions for the fcc lattice as a function of the distance (in units of the lattice constant a_{lattice}) for the bare interaction parameters of $a=2.5$, 3.5, 5, and 7.
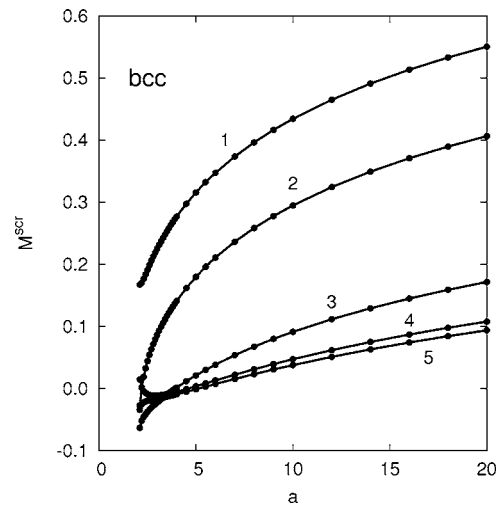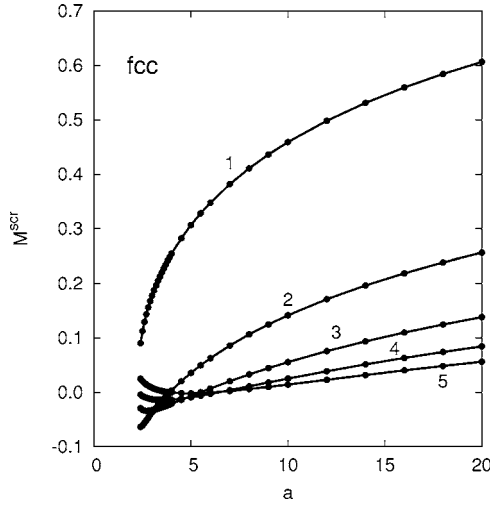
FIG. 9. Screened electrostatic interactions for the fcc lattice as a function of the bare interaction parameter a for the first five neighbors (indicated explicitly).

$$V_{ij}^{Mad} = V_{ij}^{AA} + V_{ij}^{BB} - V_{ij}^{AB} - V_{ij}^{BA} = M_{ij}^{scr}(q_i^A - q_i^B)(q_j^A - q_j^B). \tag{37}$$

For derivation see Ref. 9.

E. Distribution of local charges in random alloys

The configuration of a binary alloy A_xB_y ($y=1-x$) is characterized by a set of occupation indices $\{\eta_i^Q\}$, where $\eta_i^Q=1$ if the site i is occupied by an atom of the type Q, and $\eta_i^Q=0$ otherwise. For simplicity we will assume nonrandom interactions $a_i=a$ for all i, because a similar analysis for random interactions based on the CPA, although straightforward, is rather cumbersome. The net charge q_i at site i is, according to Eq. (7), given by

$$q_i = \sum_j G_{ij}k_j = G_{ii}k_i + \sum_j{}' G_{ij}k_j, \tag{38}$$

and the conditionally averaged net charge of atom Q by

$$\bar{q}^Q = \frac{\langle \eta_i^Q q_i \rangle}{\langle \eta_i^Q \rangle} = G_{ii}k^Q + \sum_j{}' G_{ij}\langle k \rangle, \tag{39}$$

because $\langle k_j \rangle = \langle k \rangle$ is independent of the site index j. Note that $\bar{q}^Q = G_{ii}(k^Q - \langle k \rangle)$, which follows from Eq. (16). Let us assume that the site i is occupied by an atom Q, i.e., $\eta_i^Q=1$. Then the fluctutations of the charge q_i are given by

$$\delta q_i = q_i - \bar{q}^Q = \sum_j{}' G_{ij}(k_j - \langle k \rangle). \tag{40}$$

The quantity $\Delta_j=k_j-\langle k \rangle$ is random and can attain two values, namely, $\Delta_A=y(k^A-k^B)$, with probability x, and $\Delta_B=-x(k^A-k^B)$, with probability y. The charge fluctuations,

$$\delta q_i = \sum_j{}' G_{ij}\Delta_j, \tag{41}$$

are expressed as a linear combination (with fixed nonrandom coefficients) of independent random variables. Consequently,

the δq_i are random quantities and their probabilty distribution can be calculated using the technique of characteristic functions[17] defined as

$$\chi(t) = \int_{-\infty}^{\infty} d\xi e^{i\xi t}p(\xi), \tag{42}$$

where $p(\xi)$ is the probability density of the random variable ξ. If $X_1, X_2, \ldots$ is a sequence of independent random variables whose characteristic functions are $\chi_1(t), \chi_2(t), \ldots$, and $S=A_1X_1+A_2X_2+\ldots$, where A_i are constants, the characteristic function $\chi_S(t)$ for S is given by $\chi_S(t)=\chi_1(A_1t)\chi_2(A_2t)\ldots$. The probability density of the variable Δ_j is given by

$$p(\Delta_j = \xi) = x\delta(\xi - yk_0) + y\delta(\xi + xk_0), \tag{43}$$

where $k_0=k^A-k^B$ and the characteristic function by

$$\chi_j(t) = \int_{-\infty}^{\infty} d\xi e^{i\xi t}p(\xi) = xe^{iyk_0t} + ye^{-ixk_0t}. \tag{44}$$

The characteristic function of the random quantity δq_i [Eq. (41)] is therefore given by the infinite product of characteristic functions,

$$\chi_{\delta q_i}(t) = \prod_j{}' \chi_j(G_{ij}t) = \prod_j{}'(xe^{iG_{ij}k_0yt} + ye^{-iG_{ij}k_0xt}). \tag{45}$$

It is unlikely that this infinite product can be calculated analytically, but we can find at least several first moments or cumulants of the resulting distribution. Taking the logarithm on both sides of Eq. (45) we get

$$\ln \chi_{\delta q_i}(t) = \sum_j{}' \ln[xe^{iG_{ij}k_0yt} + ye^{-iG_{ij}k_0xt}]. \tag{46}$$

By expanding $\ln \chi_{\delta q_i}(t)$ in powers of t for $|t| \ll 1$,

$$\ln \chi_{\delta q_i}(t) = \sum_{k=0}^{+\infty} \kappa_k(it)^k, \tag{47}$$

we find several first (central) cumulants

$$\kappa_0 = 0,$$

$$\kappa_1 = 0,$$

$$\kappa_2 = xyk_0^2 G^{(2)},$$

$$\kappa_3 = xy(y-x)k_0^3 G^{(3)},$$

$$\kappa_4 = xy(1-6xy)k_0^4 G^{(4)}, \tag{48}$$

where

$$G^{(n)} = \sum_j{}'(G_{ij})^n. \tag{49}$$

The odd cumulants are nonzero for $x \neq y$. Therefore, the distribution function is nonsymmetric in such a case. The distribution function is also different from the Gaussian distribution because $\kappa_n \neq 0$ for $n > 2$.

The probability density can be reconstructed only approximately from several first moments. If we employ only

the first four moments, we can use the distribution functions that belong to the Pearson system.[17] These functions fulfill the differential equation $p'(x)/p(x)=(m-x)/(a+bx+cx^2)$, which is a suitable generalization of the relation valid for the normal (Gauss) distribution law. Note that for $b=c=0$ we recover normal distribution. The four parameters a, b, c, and m can be found by demanding that the first four moments of the distribution $p(x)$ have prescribed values.

F. Total energy of an alloy

The Madelung energy of an alloy

$$E^{\text{Mad}} = \frac{1}{2}\sum_i q_i V_i \tag{50}$$

can be rewritten as

$$E^{\text{Mad}} = \frac{N}{2}(x\bar{q}^A\bar{V}^A + y\bar{q}^B\bar{V}^B) + \frac{1}{2}\sum_i (x\delta q_i^A \delta V_i^A + y\delta q_i^B \delta V_i^B), \tag{51}$$

where we used the fluctuations of the net charges and the Madelung potentials

$$\delta q_i^Q = q_i - \bar{q}^Q, \quad \delta V_i^Q = V_i - \bar{V}^Q. \tag{52}$$

The first term represents the mean-field contribution, i.e., the energy of the conditionally averaged charge $\bar{q}^Q$ in the conditionally averaged potential $\bar{V}^Q$, while the second term represents the contribution of local fluctuations of charges and potentials. Using the linear relation between the local charge and the Madelung potential [Eq. (1)], and its conditionally averaged version, we find

$$E_{\text{fluct}}^{\text{Mad}} = -\frac{N}{2}(xa^A m_2^A + ya^B m_2^B), \tag{53}$$

where m_2^Q is the second central moment of the random variable $\delta q_i^Q = q_i - \bar{q}^Q$, which is identical to the second cumulant κ_2^Q, given in Eq. (48).

The sum of local energies $E^{\text{loc}}([q_i])$ [Eq. (2)] can be expressed in the form

$$E^{\text{loc}} = \frac{N}{2}[xa^A(\bar{q}^A - b^A)^2 + ya^B(\bar{q}^B - b^B)^2]$$
$$+ \frac{1}{2}\sum_i [xa^A(\delta q_i^A)^2 + ya^B(\delta q_i^B)^2]. \tag{54}$$

Its fluctuation part can be rewritten as

$$E_{\text{fluct}}^{\text{loc}} = \frac{N}{2}(xa^A m_2^A + ya^B m_2^B). \tag{55}$$

It is important to note that both fluctuation terms, local and Madelung, cancel each other. The total energy is then finally given by
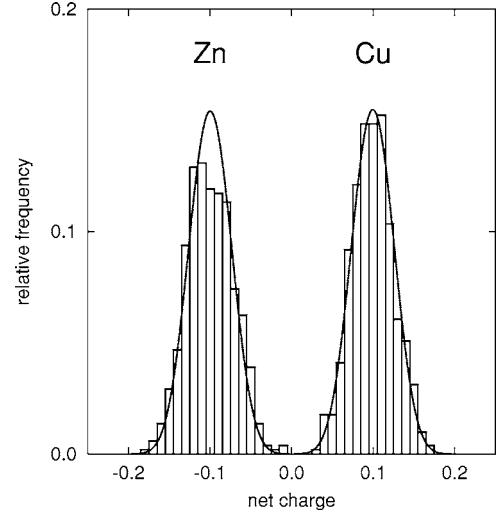

FIG. 10. Statistics of net charges in bcc $Cu_{50}Zn_{50}$ as calculated from the large supercell (Ref. 14) containing 1024 atoms (histogram) and from the cumulants, Eq. (48), using a probability density function of type I of the Pearson system (full line).

$$E^{\text{tot}} = -\frac{N}{2}[xa^A(\bar{q}^A - b^A)b^A + ya^B(\bar{q}^B - b^B)b^B]$$

$$= \frac{N}{2}(xb^A\bar{V}^A + yb^B\bar{V}^B). \tag{56}$$

III. RESULTS

A. Case study: $Cu_{50}Zn_{50}$ bcc alloy

In the following we compare the charge distribution obtained for a large supercell model of bcc-$Cu_{50}Zn_{50}$ with 1024 atoms[14] with that found from the BZW model (see Fig. 10). The basic parameters k^Q, a^Q, b^Q, and $\bar{q}^Q$ found from the supercell calculations of Ref. 14 are given in Table I.

The cumulants of the charge distribution for Cu and Zn atoms calculated from the supercell and from the present theory are compared in Table II. The agreement for Cu atoms is very good, while that for Zn atoms is less spectacular. In particular, the value of the second cumulant, which gives the width of the distribution predicted from the model, is smaller by 3.05 σ (where σ is the mean square deviation) than the value found from the supercell.

This discrepancy between the supercell and the model results is not large and at present its origin is not clear. The most probable causes are local environment effects and a possible short-range effect in the supercell that are not included in our model calculations, which assume that the al-

TABLE I. Parameters k^Q, a^Q, b^Q, and $\bar{q}^Q$ of the 1024 atom model of the $Cu_{50}Zn_{50}$ in Ref. 14.

Atom	k^Q (Ry)	a^Q (Ry)	b^Q	$\bar{q}^Q$
Cu	0.14533	1.83915	0.07902	0.099783
Zn	−0.14350	1.82082	−0.07810	−0.099783

TABLE II. Cumulants κ_n of the net-charge distribution from the supercell calculations of Ref. 14 and from the present model for bcc $Cu_{50}Zn_{50}$.

Cumulant	Cu		Zn	
	Supercell	Model	Supercell	Model
κ_2	6.35×10^{-4}	6.33×10^{-4}	7.91×10^{-4}	6.39×10^{-4}
κ_3	1.45×10^{-6}	0.0	3.26×10^{-6}	0.0
κ_4	-9.16×10^{-8}	-6.88×10^{-8}	-1.02×10^{-7}	-7.01×10^{-8}
κ_5	-3.74×10^{-9}	0.0	-4.03×10^{-9}	0.0
κ_6	-1.50×10^{-10}	3.29×10^{-11}	1.86×10^{-10}	3.39×10^{-11}

loy is completely random without any short-or long-range order. This problem deserves further attention.

IV. DISCUSSION

It is useful to compare the prescription for the Madelung potential and for the Madelung energy employed in the screened impurity model (SIM) with those given by the BZW model. All the screening charge in the SIM is concentrated to the first coordination shell and the effective Madelung potential is $\bar{V}_i = \Sigma_j^{NN} M_{ij} q_j = -e^2 q_i / R_1$, because $q_j = -q_i / Z_1$, where R_1 is the nearest-neighbor distance and Z_1 is the number of nearest-neighbor atoms. This could lead to some overestimate of the effective potential $\bar{V}_i$. However, the screening charge in the BZW model extends, at least in principle, to all coordination shells, and perhaps more importantly, the screening in the BZW model depends on the individual properties of the atomic species forming the alloy, while in the SIM no such dependence is present. Because the SIM is based on the isomorphous CPA, the contribution to the Madelung energy (up to the factor β) has the form of a mean-field contribution, i.e., the first term in Eq. (51).

On the other hand, the charge-correlated model (CCM) is a polymorphous variant of the CPA. The main approximation in the CCM is that it is limited to interactions with the nearest neighbors only, while in reality (and also in the BZW model) the interactions with all lattice sites play a role.

Both models, the SIM and the CCM, represent quite reasonable, although somewhat rough approximations of the real situation as follows from their respective comparison to the BZW model.

The BZW model can describe (although approximately) the screening phenomena in various types of solids characterized by a wide range of parameters a_i. On the other hand, in metallic alloys the screening parameters fall into a narrow interval (universal screening, cf. Refs. 9 and 10) for which $M^{scr}(R)$ can oscillate and attain negative values (see Figs. 6 and 7).

The BZW model is rather simple, its solution is straightforward, and it is based on the balance between charge transfer and local interactions. Its main limitation is that it is situated in between the isomorphous and polymorphous alloy models: it includes only those local environment effects that

are caused by electrostatic interactions, but not those caused by electronic structure effects beyond the single-site approximation, because the parameters a_i and b_i assume only the values a^Q and b^Q, which corresponds to an isomorphous alloy model.

V. CONCLUSIONS

We studied in detail the properties of the model of charge transfer in alloys proposed by Bruno, Zingales, and Wang[13] and showed that the BZW model leads to a formalism closely resembling a single-band tight-binding model of the electronic structure. We derived an expression for screened on-site interactions and discussed their relations to and differences from the Hubbard U. Furthermore, we derived an expression for screened Madelung interactions and discussed their contributions to the effective interatomic interactions in the alloy Ising Hamiltonian. It was shown that the BZW model can predict the statistics of net charges on A and B atoms in an alloy correctly. We also discussed the relations of the present approach to other theories aimed at a description of Coulomb effects within the CPA such as the SIM and the correlated-charge model (CC).

The theory is particularly simple in the case of nonrandom interactions a_i. We employed this nonrandom approximation $a^A = a^B = a$ when illustrating the properties of the Madelung matrix, nevertheless, we presented theoretical results valid for random a_i, and only in exceptional cases, in order to avoid cumbersome equations, we resorted to the nonrandom approximation. It is straightforward to include random interactions via the CPA, which we used for calculations of the Cu-Zn alloy in Sec. III A.

We expect that the present analysis in combination with the local-field CPA will bring an improved and accurate computational scheme for disordered alloys with modest requirements for computer resources.

Finally, it should be noted that the BZW model can easily be generalized to include, besides monopole-monopole interactions, also multipole interactions. This most likely leads to a more efficient screening (cf. Ref. 10).

APPENDIX: SCREENED ELECTROSTATIC INTERACTIONS

We fix the charges q_i at several lattice sites (the corresponding projection operator is denoted as P), while we leave the charges on the rest of the lattice (projector $Q = 1 - P$) to relax so as to attain the minimal energy. The charges now differ from their equilibrium values [Eq. (7)] (which we now denote as $q_i^{(0)}$) by some amount y_i

$$q_i = \sum_j G_{ij}k_j + y_i. \tag{A1}$$

The total energy (2) can now be expressed in matrix notation as

$$E = E_0 + \frac{1}{2}y^T H y = E_0 + \frac{1}{2}(y_P^T H_{PP} y_P + y_Q^T H_{QP} y_P + y_P^T H_{PQ} y_Q$$

$$+ y_Q^T H_{QQ} y_Q), \tag{A2}$$

$$E_0 = \frac{1}{2}(b^T - k^T G)k, \tag{A3}$$

where the superscript T denotes transposition. From the condition for a minimum of energy

$$\frac{\partial E}{\partial y_Q^T} = 0, \quad \text{i.e.,} \quad H_{QP}y_P + H_{QQ}y_Q = 0, \tag{A4}$$

we find

$$E_{\min} = E_0 + \frac{1}{2}k^T G \frac{P}{G_{PP}}Gk - k^T G \frac{P}{G_{PP}}Gq_P + \frac{1}{2}q_P^T \frac{P}{G_{PP}}q_P. \tag{A5}$$

The screened electrostatic interaction between two sites $i \in P$ and $j \in P$ thus reads

$$M_{ij}^{\text{scr}} = \frac{\partial^2 E_{\min}}{\partial q_i \partial q_j} = \left(\frac{P}{G_{PP}}\right)_{ij}. \tag{A6}$$

The induced charge deviations y_Q can be found from Eq. (A4),

$$y_Q = G_{QP}\frac{P}{G_{PP}}y_P, \tag{A7}$$

from which directly follows Eq. (36).

The asymptotic form of the screened electrostatic interactions for large distances can be derived from the continuous limit of the expression (A2). In the continuous limit the excess charge y_i is replaced by continuous charge density $y(\mathbf{r}) = y_i/\Omega_0$, where Ω_0 is the volume of the elementary cell. The energy (A2) is then given by

$$E^{\text{cont}} = \frac{1}{2}A \int d^3r\, y^2(\mathbf{r}) + \frac{e^2}{2}\int d^3r \int d^3r' \frac{y(\mathbf{r})y(\mathbf{r}')}{|\mathbf{r} - \mathbf{r}'|}, \tag{A8}$$

where $A = (xa^A + ya^B)\Omega_0$.

The interaction energy E^{int} of two excess point charges Q_1 and Q_2 located at $\mathbf{r}_1$ and $\mathbf{r}_2$ can be found by minimizing E^{cont} [Eq. (A8)] with respect to $y(\mathbf{r})$. This leads to the Helmholtz equation and the result is

$$E^{\text{int}} = e^2 \frac{\exp(-K|\mathbf{r} - \mathbf{r}'|)}{|\mathbf{r} - \mathbf{r}'|}Q_1 Q_2, \tag{A9}$$

where

$$K = \sqrt{\frac{4\pi e^2}{A}}. \tag{A10}$$

For example, for the Cu-Zn bcc alloy (Sec. III A) we find $K = 0.4063$ (bohr)$^{-1}$. The screened electrostatic interaction for large R is then

$$M_{ij}^{\text{scr}} = \frac{e^2}{R_{ij}}\exp(-KR_{ij}). \tag{A11}$$

---

*Electronic address: drchal@fzu.cz

[1] R. Magri, S. H. Wei, and A. Zunger, Phys. Rev. B **42**, 11388 (1990).

[2] A. V. Ruban, I. A. Abrikosov, and H. L. Skriver, Phys. Rev. B **51**, 12958 (1995).

[3] R. Zeller, J. Phys. F: Met. Phys. **17**, 2123 (1987).

[4] D. D. Johnson and F. J. Pinski, Phys. Rev. B **48**, 11553 (1993).

[5] B. Ujfalussy, J. S. Faulkner, N. Y. Moghadam, G. M. Stocks, and Y. Wang, Phys. Rev. B **61**, 12005 (2000).

[6] P. P. Singh and A. Gonis, Phys. Rev. B **49**, 1642 (1994).

[7] Y. Wang, G. M. Stocks, W. A. Shelton, D. M. C. Nicholson, Z. Szotek, and W. M. Temmerman, Phys. Rev. Lett. **75**, 2867 (1995).

[8] I. A. Abrikosov, A. M. N. Niklasson, S. I. Simak, B. Johansson, A. V. Ruban, and H. L. Skriver, Phys. Rev. Lett. **76**, 4203 (1996).

[9] A. V. Ruban and H. L. Skriver, Phys. Rev. B **66**, 024201 (2002).

[10] A. V. Ruban, S. I. Simak, P. A. Korzhavyi, and H. L. Skriver, Phys. Rev. B **66**, 024202 (2002).

[11] J. S. Faulkner, Y. Wang, and G. M. Stocks, Phys. Rev. B **52**, 17106 (1995).

[12] E. Bruno, L. Zingales, and A. Milici, Phys. Rev. B **66**, 245107 (2002).

[13] E. Bruno, L. Zingales, and Y. Wang, Phys. Rev. Lett. **91**, 166401 (2003).

[14] J. S. Faulkner, Y. Wang, and G. M. Stocks, Phys. Rev. B **55**, 7492 (1997).

[15] P. P. Ewald, Ann. Phys. **64**, 253 (1921).

[16] F. Ducastelle, *Order and Phase Stability in Alloys* (North-Holland, Amsterdam, 1991).

[17] J. F. Kenney and E. S. Keeping, *Mathematics of Statistics, Part II* (Van Nostrand, Princeton, NJ, 1951).